Published for SISSA by Springer

Received: *February 27, 2026*
Revised: *March 24, 2026*
Accepted: *April 13, 2026*
Published: *June 1, 2026*

Measurements of branching fractions of $\Lambda_c^+ \to \Sigma^0 K_S^0 \pi^+$ and $\Lambda_c^+ \to \Sigma^0 K_S^0 K^+$

The BESIII collaboration

Full author list at the end of the paper

E-mail: besiii-publications@ihep.ac.cn

Abstract: Based on a data sample corresponding to an integrated luminosity of 6.4 fb^{-1} of e^+e^- annihilation and collected with the BESIII detector at 13 center-of-mass energy points ranging between 4.600 GeV and 4.950 GeV, we report the first observation of the singly Cabibbo-suppressed decay $\Lambda_c^+ \to \Sigma^0 K_S^0 \pi^+$ with a statistical significance of 5.9σ. The branching fraction is determined to be $\mathcal{B}(\Lambda_c^+ \to \Sigma^0 K_S^0 \pi^+) = (0.58 \pm 0.14_{\text{stat.}} \pm 0.04_{\text{syst.}}) \times 10^{-3}$. In addition, the decay $\Lambda_c^+ \to \Sigma^0 K_S^0 K^+$ has also been investigated, and the evidence for this decay is obtained with a statistical significance of 3.7σ.

Keywords: Branching fraction, Charm Physics, e^+-e^- Experiments, Flavour Physics

ArXiv ePrint: 2602.22754

https://doi.org/10.1007/JHEP06(2026)009

JHEP06(2026)009

Contents

1 Introduction

The study of the dynamics of charmed baryon decays is crucial to elucidate the weak and strong interactions in the Standard Model (SM) of particle physics [1, 2]. The ground state of the singly-charmed baryon Λ_c^+ with a spin-parity $J^P = \frac{1}{2}^+$ [3] was first observed in the 1980s [4]. Since 2014, there has been notable progress on the weak hadronic decays of Λ_c^+, $\Xi_c^{+(0)}$, and Ω_c^0, both experimentally and theoretically [5–9]. This has provided crucial information about the properties of all the singly-charmed baryons and the searches for doubly-charmed baryons (Ξ_{cc} and Ω_{cc}) [10]. However, our understanding of the decay dynamics of charmed baryons is still limited, due to the lack of high-precision experimental measurements and the difficulties in the theoretical treatment of strong interaction effects.

For charmed meson decays, both the annihilation and exchange mechanisms are either helicity- or color-suppressed, so the spectator diagram is considered to be the dominant mechanism [11], and the factorization approach [12] has been successfully applied to charmed meson decays. In contrast, for charmed baryons, there is no helicity and color suppression since there is an additional light quark, so the W-exchange contributions may be large, and the factorization approximation generally does not work. Consequently, understanding W-exchange contributions is of importance for the description of non-leptonic charmed baryon decay.

To overcome these challenges [13], significant efforts have been devoted to developing alternative theoretical frameworks for charmed hadron decays [14, 15]. These approaches recognize the necessity of considering nonfactorizable effects. The SU(3) flavor symmetry ($\mathrm{SU}(3)_F$) method has been tested as a useful tool in both the beauty and charmed hadron decays [16, 17]. Its feasibility has been established in two-body and three-body semileptonic charmed baryon weak decays. The contributions of the color-antisymmetric and -symmetric part of the effective Hamiltonian have been considered and fit to experimental data points to predict the branching fractions (BF) of unknown decays [18]. Experimental investigations are of great importance in validating the theoretical methods.

JHEP06(2026)009

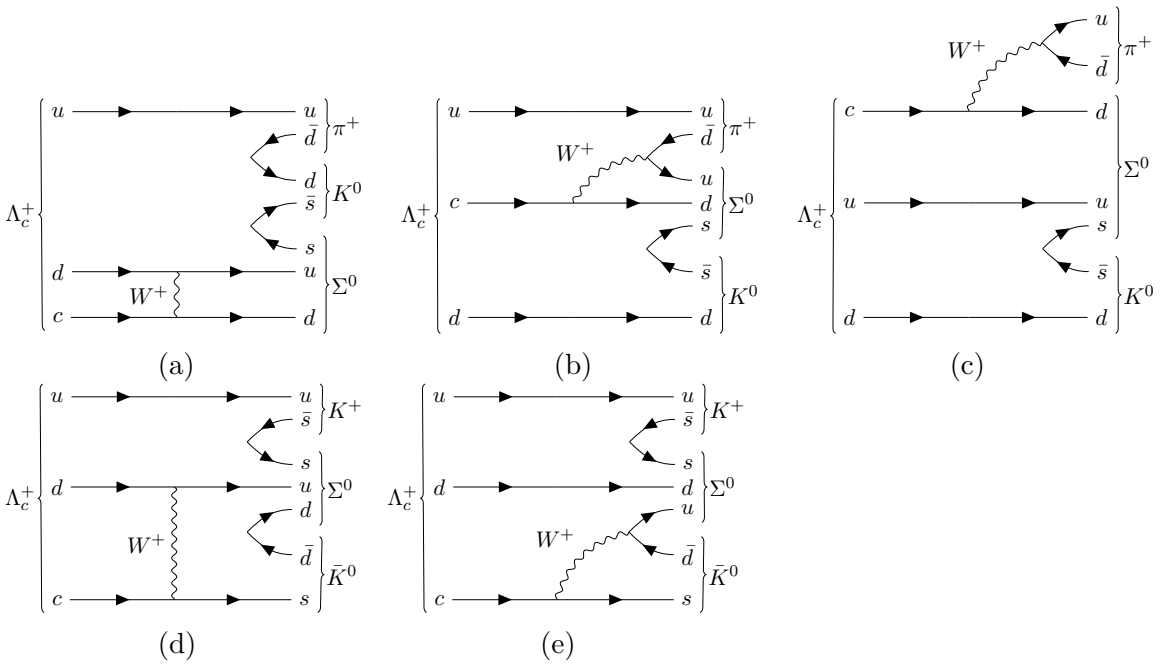

Figure 1. The (a) W-exchange diagram, (b) internal W-emission diagram, (c) external W-emission diagram for $\Lambda_c^+ \to \Sigma^0 K_S^0 \pi^+$ as well as (d) W-exchange diagram and (e) internal W-emission diagram for $\Lambda_c^+ \to \Sigma^0 K_S^0 K^+$.

The total BF of the measured Λ_c^+ decays is still only around 70% according to the Particle Data Group (PDG) [19], and many decay modes of Λ_c^+ remain unknown. An upper limit for the BF of $\Lambda_c^+ \to \Sigma^0 K_S^0 K^+$ has been determined by BESIII using the 4.5 fb^{-1} of data collected at center-of-mass energies between 4.600 and 4.700 GeV with the double tag method to be 1.28×10^{-3} at the 90% confidence level (C.L.) [20]. In this work, we use more data samples with single tag method to investigate this decay mode again. The decay $\Lambda_c^+ \to \Sigma^0 K_S^0 \pi^+$ has not been observed experimentally. Both decays involve the W-exchange and W-emission diagrams as shown in figure 1.

The Λ_c decays can have contributions from both direct nonresonant and resonant processes. The nonresonant contributions to $\Lambda_c^+ \to \Sigma^0 K_S^0 \pi^+$ and $\Lambda_c^+ \to \Sigma^0 K_S^0 K^+$ have been investigated using SU(3)$_F$ [18, 21], with the predicted BFs listed in table 1. In addition, the decay $\Lambda_c^+ \to \Sigma^0 K_S^0 K^+$ can proceed via the intermediate channel $\Lambda_c^+ \to \Sigma^0 a_0(980)^+$ [22], followed by $a_0(980)^+ \to K_S^0 K^+$. This opens a new avenue for probing light scalar mesons, especially taking into account the BESIII measurement of $\mathcal{B}(\Lambda_c^+ \to \Lambda a_0(980)^+)$ [23], which significantly exceeds theoretical predictions. Similarly, the decay $\Lambda_c^+ \to \Sigma^0 K_S^0 \pi^+$ may involve various resonant decays, such as $\Lambda_c^+ \to \Sigma^0 K^{*+}(K^{*+} \to K_S^0 \pi^+)$, $K_S^0 \Sigma^{*0}(\Sigma^{*0} \to \Sigma^0 \pi^+)$, and $\Sigma^0 K_0^*(700)^+(K_0^*(700)^+ \to K_S^0 \pi^+)$. Differences from theoretical predictions in these decays can provide valuable insights into the presence of additional resonant contributions. For instance, BESIII has observed, in addition to a nonresonant component, the decay $\Lambda_c^+ \to \Lambda K^*(892)^+$ [24] through an analysis of $\Lambda_c^+ \to \Lambda K_S^0 \pi^+$. Moreover, the reported $\mathcal{B}(\Lambda_c^+ \to \Lambda K^*(892)^+)$ is consistent with the theoretical predictions based on SU(3)$_F$ [25, 26].

JHEP06(2026)009

Decay mode	$\Lambda_c^+ \to \Sigma^0 K_S^0 \pi^+$	$\Lambda_c^+ \to \Sigma^0 K_S^0 K^+$
BF	$(0.17 \pm 0.05) \times 10^{-3}$	$(0.12 \pm 0.04) \times 10^{-3}$

Table 1. Theoretical results for nonresonant decays based on $\mathrm{SU}(3)_F$ [18].

In this work, we measure the BFs of $\Lambda_c^+ \to \Sigma^0 K_S^0 \pi^+$ and $\Lambda_c^+ \to \Sigma^0 K_S^0 K^+$ by analyzing $6.4\,\mathrm{fb}^{-1}$ of data taken at 13 energy points between $\sqrt{s} = 4.600$ and $4.950\,\mathrm{GeV}$ [27] with the BESIII detector at the BEPCII collider. The charge-conjugate processes are implicitly included throughout this paper.

2 BESIII detector and Monte Carlo simulation

The BESIII detector [28] records symmetric e^+e^- collisions provided by the BEPCII storage ring [29], which operates with a peak luminosity of $1.1 \times 10^{33}\ \mathrm{cm}^{-2}\mathrm{s}^{-1}$ in the center-of-mass energy range from 1.84 to 4.95 GeV. BESIII has collected large data samples in this energy region [30]. The cylindrical core of the BESIII detector covers 93% of the full solid angle and consists of a helium-based multilayer drift chamber (MDC), a plastic scintillator time-of-flight system (TOF), and a CsI(Tl) electromagnetic calorimeter (EMC), which are all enclosed in a superconducting solenoidal magnet providing a 1.0 T magnetic field. The solenoid is supported by an octagonal flux-return yoke with resistive plate counter muon identification modules interleaved with steel.

The charged-particle momentum resolution at 1 GeV/c is 0.5%, and the dE/dx resolution is 6% for electrons from Bhabha scattering. The EMC measures photon energies with a resolution of 2.5% (5%) at 1 GeV in the barrel (end cap) region. The time resolution in the TOF barrel region was 68 ps, while that in the end cap region is 110 ps. The end cap TOF system was upgraded in 2015 using multi-gap resistive plate chamber technology, providing a time resolution of 60 ps [31–33]. About 90% of the data used were collected after this upgrade.

Simulated data samples produced with the GEANT4-based [34] MC software, which includes the geometric and material description of the BESIII detector and the detector response, are used to determine detection efficiencies and to estimate backgrounds. The simulation models considered the beam energy spread and initial state radiation (ISR) in the e^+e^- annihilations with the generator KKMC [35, 36]. The inclusive MC sample includes the production of open charm processes, the ISR production of vector charmonium(-like) states, and the continuum processes incorporated in KKMC. The known decay modes are modeled with EVTGEN [37, 38] using BFs taken from the PDG [19], and the remaining unknown charmonium decays are modeled with LUNDCHARM [39, 40]. Final state radiation from charged final state particles is incorporated using PHOTOS [41].

For the MC production of the $e^+e^- \to \Lambda_c^+ \bar{\Lambda}_c^-$ events, the observed cross sections are taken into account, and the signal decay processes are modeled to be uniformly distributed in phase space (PHSP). All the final tracks and photons are reconstructed by the GEANT4-based [34] detector simulation package.

JHEP06(2026)009

3 Event selection and data analysis

To reconstruct the signal processes, all the final particles are selected to form the Λ_c^+ candidates. Charged tracks detected in the MDC are required to be within a polar angle (θ) range of $|\cos\theta| < 0.93$, where θ is defined with respect to the z-axis, which is the symmetry axis of the MDC. For charged tracks not originating from K_S^0 or Λ decays, the distance of closest approach to the interaction point (IP) must be less than 10 cm along the z-axis, $|V_z|$, and less than 1 cm in the transverse plane, $|V_{xy}|$.

Photon candidates are identified using isolated showers in the EMC. The deposited energy of each shower must be more than 25 MeV in the barrel region ($|\cos\theta| < 0.80$) and more than 50 MeV in the end cap region ($0.86 < |\cos\theta| < 0.92$). To exclude showers that originate from charged tracks, the angle subtended by the EMC shower and the position of the closest charged track at the EMC must be greater than 10 degrees as measured from the IP. To suppress electronic noise and showers unrelated to the event, the difference between the EMC time and the event start time is required to be within [0, 700] ns.

Particle identification (PID) for charged tracks combines measurements of the energy deposited in the MDC ($\mathrm{d}E/\mathrm{d}x$) and the flight time in the TOF to form likelihoods $\mathcal{L}(h)$ ($h = p, K, \pi$) for each hadron h hypothesis. Tracks are identified as protons when the proton hypothesis has the greatest likelihood ($\mathcal{L}(p) > \mathcal{L}(K)$ and $\mathcal{L}(p) > \mathcal{L}(\pi)$), then charged kaons and pions are identified by comparing the likelihoods for the kaon and pion hypotheses, $\mathcal{L}(K) > \mathcal{L}(\pi)$ and $\mathcal{L}(\pi) > \mathcal{L}(K)$, respectively.

The Σ^0 is reconstructed through its decay final state $\gamma\Lambda(\Lambda \to p\pi^-)$. The invariant mass of the $M(\gamma\Lambda)$ is required to be within (1.179, 1.203) GeV/c^2.

Each $\Lambda(K_S^0)$ candidate is reconstructed from two oppositely charged tracks satisfying $|V_z| < 20$ cm and $|\cos\theta| < 0.93$. The two charged tracks are assigned as $p\pi^-(\pi^+\pi^-)$ and only the proton is subjected to further PID criteria. They are constrained to originate from a common vertex by applying a vertex fit and requiring the χ^2 of a vertex fit to be less than 100. The invariant mass is required to satisfy the $1.111 < M(p\pi^-) < 1.121\,\mathrm{GeV}/c^2 (0.487 < M(\pi^+\pi^-) < 0.511\,\mathrm{GeV}/c^2)$, which corresponds to three times the standard deviation of the reconstruction resolution around the known $\Lambda(K_S^0)$ mass [19]. The decay length of the $\Lambda(K_S^0)$ candidate is required to be greater than twice the vertex resolution away from the IP.

The signal candidates are identified using the beam constrained mass $M_{\mathrm{BC}} = \sqrt{E_{\mathrm{beam}}^2/c^4 - p^2/c^2}$, where p is the momentum of reconstructed Λ_c^+ candidates in the center-of-mass frame of the e^+e^- collision. To improve the signal purity, a four-constraint (4C) kinematic fit is performed for Λ_c^+ candidates. Here, we constrain the invariant mass of recoil side of Λ_c^+ candidates to the $\bar{\Lambda}_c^-$ nominal mass [19], and the invariant masses of $\pi^+\pi^-$, $p\pi^-$ and $\gamma p\pi^-$ to the nominal masses of K_S^0, Λ and Σ^0. The candidate with the minimum χ^2_{4C} given by the 4C kinematic fit is retained for further analysis. The χ^2_{4C} requirements are optimized by using the Figure of Merit (FOM= $S/\sqrt{S+B}$), where S is the number of signal events in the region $M_{\mathrm{BC}} \in [2.282,\ 2.291]\,\mathrm{GeV}/c^2$ generated by the theoretical predicted BF and updated by our final result, B is the number of background events estimated using the inclusive MC, and S and B are normalized to the integrated luminosity of the data sample. We require $\chi^2_{\mathrm{4C}} < 29$ for $\Lambda_c^+ \to \Sigma^0 K_S^0 \pi^+$ and $\chi^2_{\mathrm{4C}} < 171$ for $\Lambda_c^+ \to \Sigma^0 K_S^0 K^+$.

JHEP06(2026)009

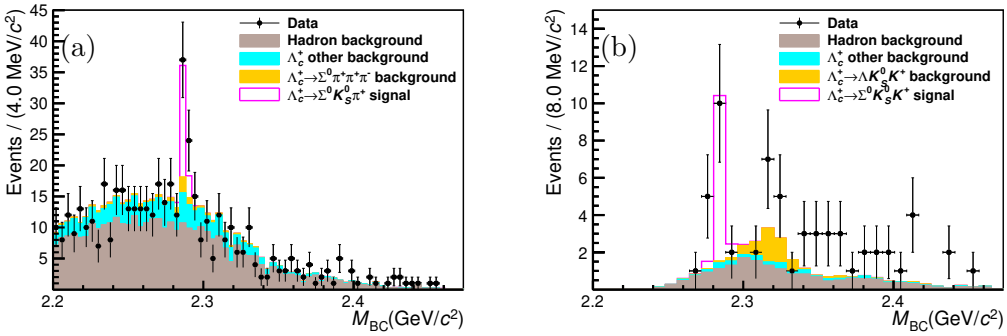

Figure 2. The $M_{\rm BC}$ distributions of the accepted candidates for (a) $\Lambda_c^+ \to \Sigma^0 K_S^0 \pi^+$ and (b) $\Lambda_c^+ \to \Sigma^0 K_S^0 K^+$. The black points with error bars are data, and the histograms are MC simulated events. The magenta, yellow, cyan, and brown histograms are the signal, peaking backgrounds, Λ_c^+ backgrounds and combinatorial backgrounds, respectively.

After all the selection criteria, the $M_{\rm BC}$ distributions for both data and inclusive MC samples are shown in figure 2. Some peaking backgrounds ($\Lambda_c^+ \to \Sigma^0\pi^+\pi^-\pi^+$ in the $\Lambda_c^+ \to \Sigma^0 K_S^0 \pi^+$ analysis and $\Lambda_c^+ \to \Lambda K_S^0 K^+$ in the $\Lambda_c^+ \to \Sigma^0 K_S^0 K^+$ analysis) are observed.

4 Determination of the branching fraction

At each energy point, the BF of the signal decay is calculated by

$$\mathcal{B} \equiv \frac{N^{\rm sig}}{2 \cdot N_{\Lambda_c^+\bar{\Lambda}_c^-} \cdot \varepsilon^{\rm sig} \cdot \mathcal{B}^{\rm inter}}, \tag{4.1}$$

where $N^{\rm sig}$ denotes the signal yield, 2 is because the charge conjugate process also contributes, $N_{\Lambda_c^+\bar{\Lambda}_c^-}$ is the number of $\Lambda_c^+\bar{\Lambda}_c^-$ events listed in table 2 and calculated using the cross section [42] and integrated luminosity [27, 43], $\varepsilon^{\rm sig}$ is the signal efficiency from the MC simulation shown in table 2 and $\mathcal{B}^{\rm inter}$ is determined by the BFs of the intermediate states ($\Sigma^0 \to \gamma\Lambda$ (100%), $\Lambda \to p\pi^-$ $(63.90 \pm 0.05)\%$ and $K_S^0 \to \pi^+\pi^-$ $(69.20 \pm 0.05)\%$)) [19].

For $\Lambda_c^+ \to \Sigma^0 K_S^0 \pi^+$, the maximum likelihood fit is performed simultaneously on the $M_{\rm BC}$ distributions of all the energy points. In the fit, the BF value is constrained to be the same at each energy point. The MC histograms for the signal shapes in figure 2 also contains some mis-reconstructed photons and mis-reconstructed π^+s and K^+s. To obtain clean signal shapes, a match based on the MC truth information is performed for signal processes using the inclusive MC sample. The angle between the reconstructed and the truth three-momenta of the tracks is required to be less than 10 degrees. The others are classified as unmatched background and provide the unmatched shape. The clean signal shapes are convolved with Gaussian functions, which account for the mass resolution difference between data and MC simulation. The parameters of the Gaussian functions are floated, but are constrained to be the same at each energy point. The background shapes are described with ARGUS functions [44] with floating parameters, except for the endpoints which are fixed by the center-of-mass energy. The ratio of unmatched backgrounds with respect to the signal

JHEP06(2026)009

$\sqrt{s}$(MeV)	$\varepsilon_{\Lambda_c^+\to\Sigma^0K_S^0\pi^+}(\%)$	$\varepsilon_{\Lambda_c^+\to\Sigma^0K_S^0K^+}(\%)$	$N_{\Lambda_c^+\bar{\Lambda}_c^-}$
4599.53	6.52±0.04	1.97±0.02	99244
4611.86	5.78±0.04	1.87±0.02	17442
4628.00	5.58±0.03	2.03±0.02	89280
4640.91	5.59±0.04	2.27±0.02	95426
4661.24	5.59±0.04	2.46±0.02	91639
4681.92	5.60±0.04	2.66±0.02	278622
4698.82	5.45±0.04	2.75±0.02	84341
4739.70	5.96±0.03	3.28±0.03	19848
4750.05	5.76±0.04	3.38±0.03	45091
4780.54	5.70±0.04	3.57±0.03	61431
4843.07	5.14±0.03	3.66±0.03	45429
4918.02	4.46±0.03	3.58±0.03	20634
4950.93	4.06±0.03	3.32±0.03	14416

Table 2. The detection efficiencies for $\Lambda_c^+ \to \Sigma^0 K_S^0 \pi^+$ and $\Lambda_c^+ \to \Sigma^0 K_S^0 K^+$, where the uncertainties are statistical only, and the number of $\Lambda_c^+\bar{\Lambda}_c^-$ events. The efficiencies do not include the BF of the sequential decay of K_S^0.

yields is fixed. For the peaking backgrounds $\Lambda_c^+ \to \Sigma^0\pi^+\pi^-\pi^+$, the yields are fixed using BFs from the PDG [19], and the shapes and efficiencies are obtained from the MC sample. By considering $N_{\Lambda_c^+\bar{\Lambda}_c^-}$, the efficiencies and BFs of intermediate states, the BF of $\Lambda_c^+ \to \Sigma^0 K_S^0\pi^+$ can be obtained. The sums of the fit plots of all energy points are shown in figure 3.

The $K_S^0\pi^+$invariant mass distribution combining 13 energy points is shown in figure 4. The $\Lambda_c^+ \to \Sigma^0 K^{*+}$ decay is seen, and the BF result is obtained by fitting the $M_{K_S^0\pi^+}$ distribution in the $M_{\rm BC}$ signal region (2.282, 2.291) GeV/c^2. Included in the fit are the contributions of $\Lambda_c^+ \to \Sigma^0 K^{*+}$, $\Lambda_c^+ \to \Sigma^0 K_S^0\pi^+$(non-$K^{*+}$), unmatched backgrounds and other backgrounds, and the shapes are obtained from MC samples. The signal shape is convolved with a Gaussian function. The mean and sigma values of the Gaussian are floated. The yields of unmatched backgrounds and other backgrounds are fixed using the result of the $M_{\rm BC}$ fit, and the yields of other components are floated. The efficiency is $(5.31 \pm 0.03)\%$.

For $\Lambda_c^+ \to \Sigma^0 K_S^0 K^+$, due to the limited statistics, all the data samples are combined in the fit process. The clean signal shape and unmatched background shape are obtained as for the $\Lambda_c^+ \to \Sigma^0 K_S^0\pi^+$ case. The parameters of the Gaussian function convolved with the clean signal shape are fixed to the values of $\Lambda_c^+ \to \Sigma^0 K_S^0\pi^+$. The background shape is described by the inclusive MC sample. The ratio of the unmatched background to the signal yield is fixed. For the peaking background $\Lambda_c^+ \to \Lambda K_S^0 K^+$, the yield is fixed by using the PDG BF [19], while the efficiency and shape are obtained from the MC sample.

The signal yields, the BF results and the significances are shown in table 3. Since the statistical significance of $\Lambda_c^+ \to \Sigma^0 K_S^0 K^+$ is only 3.7σ by comparing the fit likelihoods with

JHEP06(2026)009

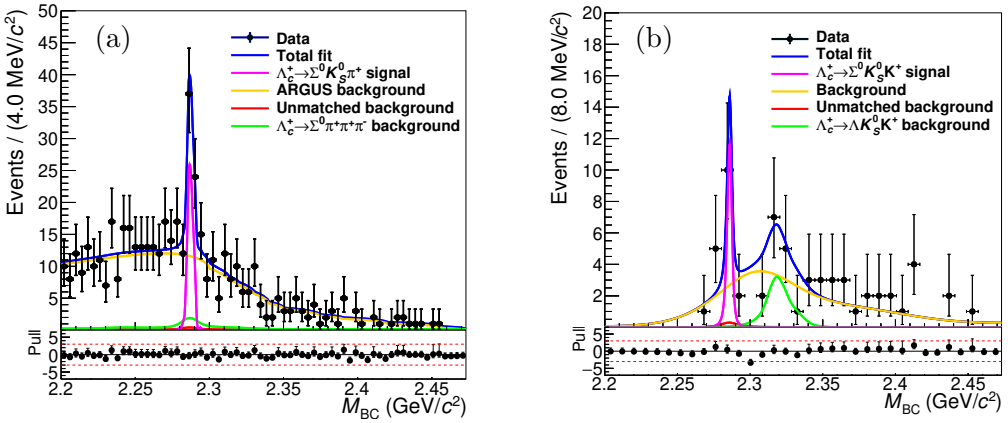

Figure 3. Results of the fits to the M_{BC} distributions for (a) $\Lambda_c^+ \to \Sigma^0 K_S^0 \pi^+$ and (b) $\Lambda_c^+ \to \Sigma^0 K_S^0 K^+$ combining 13 energy points. The black points with error bars are data, the blue, yellow, magenta, green, and red solid lines are the total fit, the ARGUS background function ($\Lambda_c^+ \to \Sigma^0 K_S^0 \pi^+$) and the MC background shape ($\Lambda_c^+ \to \Sigma^0 K_S^0 K^+$), the signals, the peaking backgrounds, and the unmatched components, respectively.

Decay mode	$N_{\rm sig}$	BFs($\times 10^{-3}$)	Statistical significance
$\Lambda_c^+ \to \Sigma^0 K_S^0 \pi^+$	28.24 ± 7.15	0.58 ± 0.14	5.9σ
$\Lambda_c^+ \to \Sigma^0 K^{*+} \to \Sigma^0 K_S^0 \pi^+$	18.48 ± 8.51	0.41 ± 0.19	2.9σ
$\Lambda_c^+ \to \Sigma^0 K_S^0 K^+$	7.92 ± 3.43	0.35 ± 0.16	3.7σ

Table 3. The signal yield, BF and significance for each decay mode, where the uncertainties are statistical only. For $\Lambda_c^+ \to \Sigma^0 K_S^0 \pi^+$ and $\Lambda_c^+ \to \Sigma^0 K_S^0 K^+$, the BF contains all resonance. For $\Lambda_c^+ \to \Sigma^0 K^{*+} \to \Sigma^0 K_S^0 \pi^+$, BF is $\mathcal{B}(\Lambda_c^+ \to \Sigma^0 K^{*+}) \times \mathcal{B}(K^{*+} \to K_S^0 \pi^+)$.

and without including the signal components, the upper limit is determined by a likelihood scan which takes into account the systematic uncertainties. The likelihood curve calculated is shown in figure 5. The upper limit at the 90% C.L. is (1.23×10^{-3}).

5 Systematic uncertainty

The systematic uncertainties on the BF measurements include contributions from the tracking, PID, K_S^0 and Λ reconstruction, photon selection, $\mathcal{B}^{\rm inter}$, χ^2_{4C} kinematic fit requirement, the fit process, MC model, the peaking and unmatched background estimation, and the number of $N_{\Lambda_c^+\bar{\Lambda}_c^-}$ events. They are summarized in table 4 and the details are described below. The total systematic uncertainties are calculated as the sum in quadrature of the individual contributions by assuming the sources are independent of one another.

- *Tracking and PID.* The systematic uncertainties associated with tracking and PID are investigated using the control samples of $e^+e^- \to K^+K^-\pi^+\pi^-$ [45]. We assign a systematic uncertainty of 1.0% for tracking and PID for each proton or charged pion. Due to the low momentum, the systematic uncertainty of tracking and PID of a charged kaon is assigned as 2.0% for each.

JHEP06(2026)009

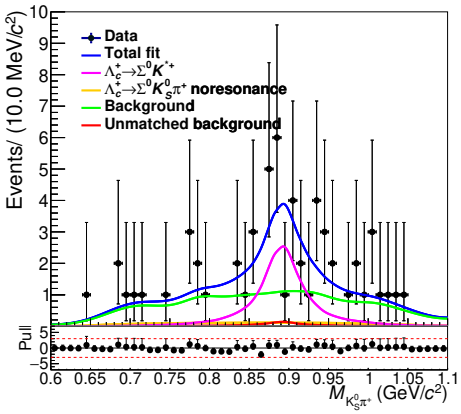

Figure 4. The fit plot of $\Lambda_c^+ \to \Sigma^0 K^{*+}$ combining 13 energy points in the $M_{\rm BC}$ signal region (2.282, 2.291) GeV/c^2. The black points with error bars are data, and the blue, magenta, yellow, red, and green lines are the total fit, signal, $\Lambda_c^+ \to \Sigma^0 K_S^0 \pi^+$(non-$K^{*+}$) process, unmatched component, and other background, respectively.

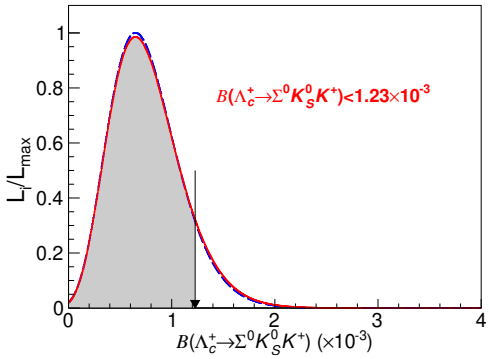

Figure 5. The likelihoods curve of $\Lambda_c^+ \to \Sigma^0 K_S^0 K^+$. The results obtained with and without incorporating the systematic uncertainties are shown in the red solid and blue dashed curves, respectively. The black arrow shows the result corresponding to the 90% C.L.

- *The K_S^0 reconstruction.* The control sample $J/\psi \to K_S^0 K^\pm \pi^\pm$ is used to study the K_S^0 reconstruction efficiency [45]. We reweight the detection efficiency of our signal process by the data-MC differences in each momentum region. The relative differences between the weighted and nominal results are assigned as the systematic uncertainties, which are 1.6% and 2.7% for $\Lambda_c^+ \to \Sigma^0 K_S^0 \pi^+$ and $\Lambda_c^+ \to \Sigma^0 K_S^0 K^+$, respectively.

- *The Λ reconstruction.* The Λ reconstruction efficiency is studied using the control sample $J/\psi \to pK^-\bar{\Lambda}$ [46], and a similar reweighting procedure as the K_S^0 reconstruction is performed. The systematic uncertainties are evaluated as the relative difference between the weighted and nominal efficiencies, which are 1.6% for $\Lambda_c^+ \to \Sigma^0 K_S^0 \pi^+$ and 2.8% for $\Lambda_c^+ \to \Sigma^0 K_S^0 K^+$.

JHEP06(2026)009

Source	$\Lambda_c^+ \to \Sigma^0 K_S^0 \pi^+$	$\Lambda_c^+ \to \Sigma^0 K_S^0 K^+$
Tracking	1.0	2.0
PID	1.0	2.0
K_S^0 reconstruction	1.6	2.7
Λ reconstruction	1.6	2.8
Photon selection	1.5	1.5
$\mathcal{B}_i^{\rm inter}$	0.8	0.8
$\chi^2_{\rm 4C}$ requirement	0.2	—
$M_{\rm BC}$ fit	2.4	8.4
MC model	1.4	—
Peaking background	5.0	1.1
Unmatched background	1.9	3.7
$N_{\Lambda_c^+ \bar{\Lambda}_c^-}$	1.6	1.4
Total	7.0	10.7

Table 4. The systematic uncertainties (%).

- *Photon selection.* The uncertainty of the photon reconstruction is studied based on the control sample $J/\psi \to \pi^+\pi^-\pi^0$ with $\pi^0 \to \gamma\gamma$. For our signal processes, the energy of the photon is around 0.1 GeV, so we assign 1.5% as the systematic uncertainty.

- *BFs of the intermediate states.* The BFs of intermediate states ($\Sigma^0 \to \Lambda\gamma, \Lambda \to p\pi^-, K_S^0 \to \pi^+\pi^-$) are used as an input in the analysis and quoted from the PDG [19]; their uncertainties are propagated, giving a systematic uncertainty of 0.8%.

- $\chi^2_{\rm 4C}$ *requirement.* The systematic uncertainty of the $\chi^2_{\rm 4C}$ requirement arises from the difference between data and MC samples. To study the effect, we fit the $\chi^2_{\rm 4C}$ distribution of data using the MC-simulated signal shape convolved with a Gaussian function with free parameters. The background shapes are obtained from the inclusive MC sample. The Gaussian parameters are used to smear the value of $\chi^2_{\rm 4C}$ of MC sample to obtain new values for the efficiency and BF. The difference with the nominal BF is assigned as the systematic uncertainty for $\Lambda_c^+ \to \Sigma^0 K_S^0 \pi^+$ process (0.15%). Due to the low statistics of $\Lambda_c^+ \to \Sigma^0 K_S^0 K^+$, we use the same Gaussian parameters as $\Lambda_c^+ \to \Sigma^0 K_S^0 \pi^+$; the resulting difference compared to the nominal BF is found to be negligible.

- $M_{\rm BC}$ *fit.* The systematic uncertainty of the $M_{\rm BC}$ fit includes those associated with the signal and background shapes. The uncertainty associated with the signal MC shape is estimated by changing it to the Crystal Ball function. The uncertainty due to the background shape of $\Lambda_c^+ \to \Sigma^0 K_S^0 \pi^+$ is estimated with an alternative background shape obtained from the inclusive MC sample. The total systematic uncertainty is estimated to be 2.4%. For $\Lambda_c^+ \to \Sigma^0 K_S^0 K^+$, the background shapes are obtained from inclusive MC samples. Here we change it to the Crystal Ball function with parameters obtained from the fit to the background MC sample. The total systematic uncertainty is estimated to be 8.4%.

JHEP06(2026)009

- *MC model.* Due to limited statistics, we only use the PHSP model to generate the signal process. For $\Lambda_c^+ \to \Sigma^0 K_S^0 \pi^+$, we find evidence for the $\Lambda_c^+ \to \Sigma^0 K^{*+}$ process from the $K_S^0\pi^+$ mass distribution of data. Therefore, we include this process in the signal MC generation. The fraction of $\Lambda_c^+ \to \Sigma^0 K^{*+}$ in the generator is obtained by fitting the $K_S^0\pi^+$ mass distribution. The BF difference obtained by varying the input fraction by $\pm1\sigma$ is assigned as the systematic uncertainty (1.4%). For $\Lambda_c^+ \to \Sigma^0 K_S^0 K^+$, no significant resonance is observed and the MC simulation models data well. So the systematic uncertainty of the MC model is ignored.

- *Peaking background.* In the nominal analysis, the yields of the peaking backgrounds are estimated with the efficiency and the BF quoted from the PDG. The input BFs are varied by $\pm1\sigma$ in the fit, and the largest change of the re-measured BF is taken as the systematic uncertainty, which is 5.0% for $\Lambda_c^+ \to \Sigma^0 K_S^0 \pi^+$ and 1.1% for $\Lambda_c^+ \to \Sigma^0 K_S^0 K^+$.

- *The unmatched background.* To estimate the uncertainty caused by the angle requirement, we vary it by 5 degrees and obtain a new BF. The BF difference is assigned as the systematic uncertainty, which is 1.9% for $\Lambda_c^+ \to \Sigma^0 K_S^0 \pi^+$ and 3.7% for $\Lambda_c^+ \to \Sigma^0 K_S^0 K^+$.

- *The number of $N_{\Lambda_c^+\bar{\Lambda}_c^-}$ events.* $N_{\Lambda_c^+\bar{\Lambda}_c^-}$ is obtained by the luminosity [27, 43] and the cross section [42]. Its systematic uncertainty is estimated to be 1.6% for $\Lambda_c^+ \to \Sigma^0 K_S^0 \pi^+$ and 1.4% for $\Lambda_c^+ \to \Sigma^0 K_S^0 K^+$.

6 Summary

By analyzing 6.4 fb^{-1} of e^+e^- annihilation data collected at center-of-mass energies ranging from $\sqrt{s} = 4.600 - 4.950$GeV with the BESIII detector, we report the first observation of $\Lambda_c^+ \to \Sigma^0 K_S^0 \pi^+$ with a statistical significance of 5.9σ. The measured branching fraction exhibits a notable difference compared to the theoretical prediction, listed in table 5, which excludes resonant contributions. The resonance contribution of $\Lambda_c^+ \to \Sigma^0 K^{*+}$ is evident in figure 4, albeit with low significance. The BF result is $\mathcal{B}(\Lambda_c^+ \to \Sigma^0 K^{*+}) \times \mathcal{B}(K^{*+} \to K_S^0\pi^+) = (0.41 \pm 0.19 \pm 0.03) \times 10^{-3}$, by considering the systematic uncertainty similar to $\Lambda_c^+ \to \Sigma^0 K_S^0 \pi^+$. The resonant contribution plays a very significant role in the $\Lambda_c^+ \to \Sigma^0 K_S^0 \pi^+$ decay.

Furthermore, the BF for the decay channel $\Lambda_c^+ \to \Sigma^0 K_S^0 K^+$ has been measured with a statistical significance of 3.7σ. We establish an upper limit at the 90% C.L. on the branching fraction to be $\mathcal{B}(\Lambda_c^+ \to \Sigma^0 K_S^0 K^+) < 1.23 \times 10^{-3}$. This result is consistent with both theoretical expectations [18] and the previous BESIII measurement [20] (table 5). These findings provide crucial experimental constraints for understanding the decay dynamics and internal structure of the ground-state charmed baryon Λ_c^+.

Acknowledgments

We thank Y. K. Hsiao for useful discussions. The BESIII Collaboration thanks the staff of BEPCII (https://cstr.cn/31109.02.BEPC) and the IHEP computing center for their strong support. This work is supported in part by National Key R&D Program of China under Contracts Nos. 2023YFA1606000, 2023YFA1606704, 2023YFA1609400; National Natural

JHEP06(2026)009

Decay mode	$\Lambda_c^+ \to \Sigma^0 K_S^0 \pi^+$	$\Lambda_c^+ \to \Sigma^0 K^{*+} (K^{*+} \to K_S^0 \pi^+)$	$\Lambda_c^+ \to \Sigma^0 K_S^0 K^+$
Theory calculations	(0.17 ± 0.05) [18]	(0.40 ± 0.10) [25]	(0.12 ± 0.04) [18]
Experimental results	—	—	< 1.28 [20]
This work	$(0.58 \pm 0.14_{\text{stat.}} \pm 0.04_{\text{syst.}})$	$(0.41 \pm 0.19 \pm 0.03)$	$(0.35 \pm 0.16_{\text{stat.}} \pm 0.04_{\text{syst.}})$ < 1.23

Table 5. Comparison of branching fractions between experimental results and theoretical predictions which exclude resonant production (in unit of 10^{-3}). The BF results of this work contain all resonance.

Science Foundation of China (NSFC) under Contracts Nos. 12305105, 12205141, 12105127, 11635010, 11935015, 11935016, 11935018, 12025502, 12035009, 12035013, 12061131003, 12192260, 12192261, 12192262, 12192263, 12192264, 12192265, 12221005, 12225509, 12235017, 12342502, 12361141819; the Chinese Academy of Sciences (CAS) Large-Scale Scientific Facility Program; The Strategic Priority Research Program of Chinese Academy of Sciences under Contract No. XDA0480600; CAS under Contract No. YSBR-101; Natural Science Foundation of Shandong Province under Grants No. ZR2023QA119; 100 Talents Program of CAS; The Institute of Nuclear and Particle Physics (INPAC) and Shanghai Key Laboratory for Particle Physics and Cosmology; ERC under Contract No. 758462; German Research Foundation DFG under Contract No. FOR5327; Istituto Nazionale di Fisica Nucleare, Italy; Knut and Alice Wallenberg Foundation under Contracts Nos. 2021.0174, 2021.0299, 2023.0315; Ministry of Development of Turkey under Contract No. DPT2006K-120470; National Research Foundation of Korea under Contract No. NRF-2022R1A2C1092335; National Science and Technology fund of Mongolia; Polish National Science Centre under Contract No. 2024/53/B/ST2/00975; STFC (United Kingdom); Swedish Research Council under Contract No. 2019.04595; U.S. Department of Energy under Contract No. DE-FG02-05ER41374.

Data Availability Statement. This article has no associated data or the data will not be deposited.

Code Availability Statement. This article has no associated code or the code will not be deposited.

References

[1] H.D. Politzer, *Reliable perturbative results for strong interactions?*, *Phys. Rev. Lett.* **30** (1973) 1346 [INSPIRE].

[2] D.J. Gross and F. Wilczek, *Ultraviolet behavior of non-Abelian gauge theories*, *Phys. Rev. Lett.* **30** (1973) 1343 [INSPIRE].

[3] BESIII collaboration, *Determination of the Λ_c^+ spin via the reaction $e^+e^- \to \Lambda_c^+ \bar{\Lambda}_c^-$*, *Phys. Rev. D* **103** (2021) L091101 [arXiv:2011.00396] [INSPIRE].

JHEP06(2026)009

[4] G.S. Abrams et al., *Observation of charmed baryon production in e^+e^- annihilation*, *Phys. Rev. Lett.* **44** (1980) 10 [INSPIRE].

[5] H.-Y. Cheng, *Charmed baryons circa 2015*, *Front. Phys. (Beijing)* **10** (2015) 101406 [INSPIRE].

[6] H.-Y. Cheng, *Charmed baryon physics circa 2021*, *Chin. J. Phys.* **78** (2022) 324 [arXiv:2109.01216] [INSPIRE].

[7] H.-B. Li and X.-R. Lyu, *Study of the standard model with weak decays of charmed hadrons at BESIII*, *Natl. Sci. Rev.* **8** (2021) nwab181 [arXiv:2103.00908] [INSPIRE].

[8] P.-R. Li, X.-R. Lyu and Y. Zheng, *Experimental overview on the charmed baryon decays**, *Chin. Phys. C* **50** (2026) 022002 [arXiv:2509.19141] [INSPIRE].

[9] H.-J. Wang et al., *Remarks on strong phase shifts in weak nonleptonic baryon decays*, *Sci. Bull.* **70** (2025) 1183 [arXiv:2412.02170] [INSPIRE].

[10] F.-S. Yu et al., *Discovery potentials of doubly charmed baryons*, *Chin. Phys. C* **42** (2018) 051001 [arXiv:1703.09086] [INSPIRE].

[11] T. Uppal, R.C. Verma and M.P. Khanna, *Constituent quark model analysis of weak mesonic decays of charm baryons*, *Phys. Rev. D* **49** (1994) 3417 [INSPIRE].

[12] G. Tetlalmatzi-Xolocotzi, *QCDF amplitudes from $SU(3)$ symmetries*, *PoS* **DISCRETE2022** (2024) 040 [INSPIRE].

[13] P. Zenczykowski, *Quark and pole models of nonleptonic decays of charmed baryons*, *Phys. Rev. D* **50** (1994) 402 [hep-ph/9309265] [INSPIRE].

[14] H.-Y. Cheng and B. Tseng, *Nonleptonic weak decays of charmed baryons*, *Phys. Rev. D* **46** (1992) 1042 [*Erratum ibid.* **55** (1997) 1697] [INSPIRE].

[15] H.-Y. Cheng, X.-W. Kang and F. Xu, *Singly Cabibbo-suppressed hadronic decays of Λ_c^+*, *Phys. Rev. D* **97** (2018) 074028 [arXiv:1801.08625] [INSPIRE].

[16] M.J. Savage and R.P. Springer, *$SU(3)$ predictions for charmed baryon decays*, *Phys. Rev. D* **42** (1990) 1527 [INSPIRE].

[17] C.Q. Geng, Y.K. Hsiao, C.-W. Liu and T.-H. Tsai, *Charmed baryon weak decays with $SU(3)$ flavor symmetry*, *JHEP* **11** (2017) 147 [arXiv:1709.00808] [INSPIRE].

[18] C.-Q. Geng, C.-W. Liu and S.-L. Liu, *Nonleptonic three-body charmed baryon weak decays with H(15)*, *Phys. Rev. D* **109** (2024) 093002 [arXiv:2403.06469] [INSPIRE].

[19] Particle Data Group collaboration, *Review of particle physics*, *Phys. Rev. D* **110** (2024) 030001 [INSPIRE].

[20] BESIII collaboration, *Measurement of the branching fractions of the Cabibbo-favored decays $\Lambda_c^+ \to \Lambda K_S^0 K^+$ and $\Lambda_c^+ \to \Xi^0 K_S^0 \pi^+$ and search for $\Lambda_c^+ \to \Sigma^0 K_S^0 K^+$*, *Phys. Rev. D* **112** (2025) 032006 [arXiv:2506.02969] [INSPIRE].

[21] C.Q. Geng, Y.K. Hsiao, C.-W. Liu and T.-H. Tsai, *Three-body charmed baryon decays with $SU(3)$ flavor symmetry*, *Phys. Rev. D* **99** (2019) 073003 [arXiv:1810.01079] [INSPIRE].

[22] Y.L. Wang and Y.K. Hsiao, *Charmed Λ_c^+ baryon decays into light scalar mesons in the topological $SU(3)_f$ framework*, *JHEP* **03** (2026) 216 [arXiv:2505.21311] [INSPIRE].

[23] BESIII collaboration, *Observation of $\Lambda_c^+ \to \Lambda a_0(980)^+$ and evidence for $\Sigma(1380)^+$ in $\Lambda_c^+ \to \Lambda \pi^+ \eta$*, *Phys. Rev. Lett.* **134** (2025) 021901 [arXiv:2407.12270] [INSPIRE].

JHEP06(2026)009

[24] BESIII collaboration, *Measurement of the branching fractions of the decays $\Lambda_c^+ \to \Lambda K_S^0 K^+$, $\Lambda_c^+ \to \Lambda K_S^0 \pi^+$ and $\Lambda_c^+ \to \Lambda K^{*+}$*, *Phys. Rev. D* **111** (2025) 012014 [arXiv:2410.16912] [INSPIRE].

[25] Y.K. Hsiao, Y. Yao and H.J. Zhao, *Two-body charmed baryon decays involving vector meson with $SU(3)$ flavor symmetry*, *Phys. Lett. B* **792** (2019) 35 [arXiv:1902.08783] [INSPIRE].

[26] C.Q. Geng, C.-W. Liu and T.-H. Tsai, *Charmed baryon weak decays with vector mesons*, *Phys. Rev. D* **101** (2020) 053002 [arXiv:2001.05079] [INSPIRE].

[27] BESIII collaboration, *Luminosities and energies of e^+e^- collision data taken between $\sqrt{s} = 4.61$ GeV and 4.95 GeV at BESIII*, *Chin. Phys. C* **46** (2022) 113003 [arXiv:2205.04809] [INSPIRE].

[28] BESIII collaboration, *Design and construction of the BESIII detector*, *Nucl. Instrum. Meth. A* **614** (2010) 345 [arXiv:0911.4960] [INSPIRE].

[29] C. Yu et al., *BEPCII performance and beam dynamics studies on luminosity*, in the proceedings of the *7th International Particle Accelerator Conference*, Busan, South Korea, May 08–13 (2016) [DOI:10.18429/JACoW-IPAC2016-TUYA01] [INSPIRE].

[30] BESIII collaboration, *Future physics programme of BESIII*, *Chin. Phys. C* **44** (2020) 040001 [arXiv:1912.05983] [INSPIRE].

[31] X. Li et al., *Study of MRPC technology for BESIII endcap-TOF upgrade*, *Radiat. Detect. Technol. Methods* **1** (2017) 13 [INSPIRE].

[32] Y.-X. Guo et al., *The study of time calibration for upgraded end cap TOF of BESIII*, *Radiat. Detect. Technol. Methods* **1** (2017) 15 [INSPIRE].

[33] P. Cao et al., *Design and construction of the new BESIII endcap Time-of-Flight system with MRPC technology*, *Nucl. Instrum. Meth. A* **953** (2020) 163053 [INSPIRE].

[34] GEANT4 collaboration, *GEANT4 — a simulation toolkit*, *Nucl. Instrum. Meth. A* **506** (2003) 250 [INSPIRE].

[35] S. Jadach, B.F.L. Ward and Z. Was, *Coherent exclusive exponentiation for precision Monte Carlo calculations*, *Phys. Rev. D* **63** (2001) 113009 [hep-ph/0006359] [INSPIRE].

[36] S. Jadach, B.F.L. Ward and Z. Was, *The precision Monte Carlo event generator KK for two fermion final states in e^+e^- collisions*, *Comput. Phys. Commun.* **130** (2000) 260 [hep-ph/9912214] [INSPIRE].

[37] D.J. Lange, *The EvtGen particle decay simulation package*, *Nucl. Instrum. Meth. A* **462** (2001) 152 [INSPIRE].

[38] R.-G. Ping, *Event generators at BESIII*, *Chin. Phys. C* **32** (2008) 599 [INSPIRE].

[39] J.C. Chen et al., *Event generator for J/ψ and $\psi(2S)$ decay*, *Phys. Rev. D* **62** (2000) 034003 [INSPIRE].

[40] R.-L. Yang, R.-G. Ping and H. Chen, *Tuning and validation of the Lundcharm model with J/ψ decays*, *Chin. Phys. Lett.* **31** (2014) 061301 [INSPIRE].

[41] E. Barberio, B. van Eijk and Z. Was, *PHOTOS: a universal Monte Carlo for QED radiative corrections in decays*, *Comput. Phys. Commun.* **66** (1991) 115 [INSPIRE].

[42] BESIII collaboration, *Measurement of energy-dependent pair-production cross section and electromagnetic form factors of a charmed baryon*, *Phys. Rev. Lett.* **131** (2023) 191901 [arXiv:2307.07316] [INSPIRE].

JHEP06(2026)009

[43] BESIII collaboration, *Precision measurement of the integrated luminosity of the data taken by BESIII at center of mass energies between 3.810 GeV and 4.600 GeV*, *Chin. Phys. C* **39** (2015) 093001 [arXiv:1503.03408] [INSPIRE].

[44] ARGUS collaboration, *Search for hadronic $b \to u$ decays*, *Phys. Lett. B* **241** (1990) 278 [INSPIRE].

[45] BESIII collaboration, *Study of the decays $D_s^+ \to K_S^0 K^+$ and $K_L^0 K^+$*, *Phys. Rev. D* **99** (2019) 112005 [arXiv:1903.04164] [INSPIRE].

[46] BESIII collaboration, *Measurement of absolute branching fraction of the inclusive decay $\Lambda_c^+ \to \Lambda + X$*, *Phys. Rev. Lett.* **121** (2018) 062003 [arXiv:1803.05706] [INSPIRE].

JHEP06(2026)009

The BESIII collaboration

M. Ablikim[1], M.N. Achasov[4,a], P. Adlarson[81], X.C. Ai[87], C.S. Akondi[31a,31b], R. Aliberti[39], A. Amoroso[80a,80c], Q. An[64,77,†], Y.H. An[87], Y. Bai[62], O. Bakina[40], Y. Ban[50,b], H.-R. Bao[70], X.L. Bao[49], V. Batozskaya[1,48], K. Begzsuren[35], N. Berger[39], M. Berlowski[48], M.B. Bertani[30a], D. Bettoni[31a], F. Bianchi[80a,80c], E. Bianco[80a,80c], A. Bortone[80a,80c], I. Boyko[40], R.A. Briere[5], A. Brueggemann[74], H. Cai[82], M.H. Cai[42,c,d], X. Cai[1,64], A. Calcaterra[30a], G.F. Cao[1,70], N. Cao[1,70], S.A. Cetin[68a], X.Y. Chai[50,b], J.F. Chang[1,64], T.T. Chang[47], G.R. Che[47], Y.Z. Che[1,64,70], C.H. Chen[10], Chao Chen[1], G. Chen[1], H.S. Chen[1,70], H.Y. Chen[20], M.L. Chen[1,64,70], S.J. Chen[46], S.M. Chen[67], T. Chen[1,70], W. Chen[49], X.R. Chen[34,70], X.T. Chen[1,70], X.Y. Chen[12,e], Y.B. Chen[1,64], Y.Q. Chen[16], Z.K. Chen[65], J. Cheng[49], L.N. Cheng[47], S.K. Choi[11], X. Chu[12,e], G. Cibinetto[31a], F. Cossio[80c], J. Cottee-Meldrum[69], H.L. Dai[1,64], J.P. Dai[85], X.C. Dai[67], A. Dbeyssi[19], R. E. de Boer[3], F. De Mori[80a,80c], D. Dedovich[40], C.Q. Deng[78], Z.Y. Deng[1], A. Denig[39], I. Denisenko[40], M. Destefanis[80a,80c], X.X. Ding[50,b], Y. Ding[44], Y.X. Ding[32], Yi. Ding[38], J. Dong[1,64], L.Y. Dong[1,70], M.Y. Dong[1,64,70], X. Dong[82], M.C. Du[1], S.X. Du[87], Shaoxu Du[12,e], X.L. Du[12,e], Y.Q. Du[82], Y.Y. Duan[60], Z.H. Duan[46], P. Egorov[40,f], G.F. Fan[46], J.J. Fan[20], Y.H. Fan[49], J. Fang[1,64], Jin Fang[65], S.S. Fang[1,70], W.X. Fang[1], Y.Q. Fang[1,64,†], L. Fava[80b,80c], F. Feldbauer[3], G. Felici[30a], C.Q. Feng[64,77], J.H. Feng[16], L. Feng[42,c,d], Q.X. Feng[42,c,d], Y.T. Feng[64,77], M. Fritsch[3], C.D. Fu[1], J.L. Fu[70], Y.W. Fu[1,70], H. Gao[70], Y. Gao[64,77], Y.N. Gao[50,b], Y.Y. Gao[32], Yunong Gao[20], Z. Gao[47], S. Garbolino[80c], I. Garzia[31a,31b], L. Ge[62], P.T. Ge[20], Z.W. Ge[46], C. Geng[65], E.M. Gersabeck[73], A. Gilman[75], K. Goetzen[13], J. Gollub[3], J.B. Gong[1,70], J.D. Gong[38], L. Gong[44], W.X. Gong[1,64], W. Gradl[39], S. Gramigna[31a,31b], M. Greco[80a,80c], M.D. Gu[55], M.H. Gu[1,64], C.Y. Guan[1,70], A.Q. Guo[34], H. Guo[54], J.N. Guo[12,e], L.B. Guo[45], M.J. Guo[54], R.P. Guo[53], X. Guo[54], Y.P. Guo[12,e], Z. Guo[64,77], A. Guskov[40,f], J. Gutierrez[29], N. Hüsken[39], J.Y. Han[64,77], T.T. Han[1], X. Han[64,77], F. Hanisch[3], K.D. Hao[64,77], X.Q. Hao[20], F.A. Harris[71], C.Z. He[50,b], K.K. He[60], K.L. He[1,70], F.H. Heinsius[3], C.H. Heinz[39], Y.K. Heng[1,64,70], C. Herold[66], P.C. Hong[38], G.Y. Hou[1,70], X.T. Hou[1,70], Y.R. Hou[70], Z.L. Hou[1], H.M. Hu[1,70], J.F. Hu[61,g], Q.P. Hu[64,77], S.L. Hu[12,e], T. Hu[1,64,70], Y. Hu[1], Y.X. Hu[82], Z.M. Hu[65], G.S. Huang[64,77], K.X. Huang[65], L.Q. Huang[34,70], P. Huang[46], X.T. Huang[54], Y.P. Huang[1], Y.S. Huang[65], T. Hussain[79], N. in der Wiesche[74], J. Jackson[29], Q. Ji[1], Q.P. Ji[20], W. Ji[1,70], X.B. Ji[1,70], X.L. Ji[1,64], Y.Y. Ji[1], L.K. Jia[70], X.Q. Jia[54], D. Jiang[1,70], H.B. Jiang[82], P.C. Jiang[50,b], S.J. Jiang[10], X.S. Jiang[1,64,70], Y. Jiang[70], J.B. Jiao[54], J.K. Jiao[38], Z. Jiao[25], L.C.L. Jin[1], S. Jin[46], Y. Jin[72], M.Q. Jing[1,70], X.M. Jing[70], T. Johansson[81], W. Kühn[41], S. Kabana[36], X.L. Kang[10], X.S. Kang[44], B.C. Ke[87], V. Khachatryan[29], A. Khoukaz[74], O.B. Kolcu[68a], B. Kopf[3], L. Kröger[74], L. Krümmel[3], Y.Y. Kuang[78], M. Kuessner[3], X. Kui[1,70], N. Kumar[28], A. Kupsc[48,81], Q. Lan[78], W.N. Lan[20], T.T. Lei[64,77], M. Lellmann[39], T. Lenz[39], C. Li[51], C.H. Li[45], C.K. Li[47], Chunkai Li[21], Cong Li[47], D.M. Li[87], F. Li[1,64], G. Li[1], H.B. Li[1,70], H.J. Li[20], H.L. Li[87], H.N. Li[61,g], H.P. Li[47], Hui Li[47], J.S. Li[65], J.W. Li[54], K. Li[1], K.L. Li[42,c,d], L.J. Li[1,70], Lei Li[52], M.H. Li[47], M.R. Li[1,70], M.T. Li[54], P.L. Li[70], P.R. Li[42,c,d], Q.M. Li[1,70], Q.X. Li[54], R. Li[18,34], S. Li[87], S.X. Li[12], S.Y. Li[87],

JHEP06(2026)009

Shanshan Li[27,h], T. Li[54], T.Y. Li[47], W.D. Li[1,70], W.G. Li[1,†], X. Li[1,70], X.H. Li[64,77], X.K. Li[50,b], X.L. Li[54], X.Y. Li[1,9], X.Z. Li[65], Y. Li[20], Y.G. Li[70], Y.P. Li[38], Z.H. Li[42], Z.J. Li[65], Z.L. Li[87], Z.X. Li[47], Z.Y. Li[85], C. Liang[46], H. Liang[64,77], Y.F. Liang[59], Y.T. Liang[34,70], G.R. Liao[14], L.B. Liao[65], M.H. Liao[65], Y.P. Liao[1,70], J. Libby[28], A. Limphirat[66], C.C. Lin[60], D.X. Lin[34,70], T. Lin[1], B.J. Liu[1], B.X. Liu[82], C. Liu[38], C.X. Liu[1], F. Liu[1], F.H. Liu[58], Feng Liu[6], G.M. Liu[61,g], H. Liu[42,c,d], H.B. Liu[15], H.M. Liu[1,70], Huihui Liu[22], J.B. Liu[64,77], J.J. Liu[21], K. Liu[42,c,d], K.Y. Liu[44], Ke Liu[23], Kun Liu[78], L. Liu[42], L.C. Liu[47], Lu Liu[47], M.H. Liu[38], P.L. Liu[54], Q. Liu[70], S.B. Liu[64,77], T. Liu[1], W.M. Liu[64,77], W.T. Liu[43], X. Liu[42,c,d], X.K. Liu[42,c,d], X.L. Liu[12,e], X.P. Liu[12,e], X.Y. Liu[82], Y. Liu[42,c,d], Y.B. Liu[47], Yi Liu[87], Z.A. Liu[1,64,70], Z.D. Liu[83], Z.L. Liu[78], Z.Q. Liu[54], Z.Y. Liu[42], X.C. Lou[1,64,70], H.J. Lu[25], J.G. Lu[1,64], X.L. Lu[16], Y. Lu[7], Y.H. Lu[1,70], Y.P. Lu[1,64], Z.H. Lu[1,70], C.L. Luo[45], J.R. Luo[65], J.S. Luo[1,70], M.X. Luo[86], T. Luo[12,e], X.L. Luo[1,64], Z.Y. Lv[23], X.R. Lyu[70,i], Y.F. Lyu[47], Y.H. Lyu[87], F.C. Ma[44], H.L. Ma[1], Heng Ma[27,h], J.L. Ma[1,70], L.L. Ma[54], L.R. Ma[72], Q.M. Ma[1], R.Q. Ma[1,70], R.Y. Ma[20], T. Ma[64,77], X.T. Ma[1,70], X.Y. Ma[1,64], Y.M. Ma[34], F.E. Maas[19], I. MacKay[75], M. Maggiora[80a,80c], S. Malde[75], Q.A. Malik[79], H.X. Mao[42,c,d], Y.J. Mao[50,b], Z.P. Mao[1], S. Marcello[80a,80c], A. Marshall[69], F.M. Melendi[31a,31b], Y.H. Meng[70], Z.X. Meng[72], G. Mezzadri[31a], H. Miao[1,70], T.J. Min[46], R.E. Mitchell[29], X.H. Mo[1,64,70], B. Moses[29], N.Yu. Muchnoi[4,a], J. Muskalla[39], Y. Nefedov[40], F. Nerling[19,j], H. Neuwirth[74], Z. Ning[1,64], S. Nisar[33,k], Q.L. Niu[42,c,d], W.D. Niu[12,e], Y. Niu[54], C. Normand[69], S.L. Olsen[11,70], Q. Ouyang[1,64,70], L. Pöpping[3], S. Pacetti[30b,30c], X. Pan[60], Y. Pan[62], A. Pathak[11], Y.P. Pei[64,77], M. Pelizaeus[3], G.L. Peng[64,77], H.P. Peng[64,77], X.J. Peng[42,c,d], Y.Y. Peng[42,c,d], K. Peters[13,j], K. Petridis[69], J.L. Ping[45], R.G. Ping[1,70], S. Plura[39], V. Prasad[38], F.Z. Qi[1], H.R. Qi[67], M. Qi[46], S. Qian[1,64], W.B. Qian[70], C.F. Qiao[70], J.H. Qiao[20], J.J. Qin[78], J.L. Qin[60], L.Q. Qin[14], L.Y. Qin[64,77], P.B. Qin[78], X.P. Qin[43], X.S. Qin[54], Z.H. Qin[1,64], J.F. Qiu[1], Z.H. Qu[78], J. Rademacker[69], C.F. Redmer[39], A. Rivetti[80c], M. Rolo[80c], G. Rong[1,70], S.S. Rong[1,70], F. Rosini[30b,30c], Ch. Rosner[19], M.Q. Ruan[1,64], N. Salone[48,l], A. Sarantsev[40,m], Y. Schelhaas[39], M. Schernau[36], K. Schoenning[81], M. Scodeggio[31a], W. Shan[26], X.Y. Shan[64,77], Z.J. Shang[42,c,d], J.F. Shangguan[17], L.G. Shao[1,70], M. Shao[64,77], C.P. Shen[12,e], H.F. Shen[1,9], W.H. Shen[70], X.Y. Shen[1,70], B.A. Shi[70], Ch.Y. Shi[85,n], H. Shi[64,77], J.L. Shi[8,o], J.Y. Shi[1], M.H. Shi[87], S.Y. Shi[78], X. Shi[1,64], H.L. Song[64,77], J.J. Song[20], M.H. Song[42], T.Z. Song[65], W.M. Song[38], Y.X. Song[50,b,p], Zirong Song[27,h], S. Sosio[80a,80c], S. Spataro[80a,80c], S Stansilaus[75], F. Stieler[39], M. Stolte[3], S.S Su[44], G.B. Sun[82], G.X. Sun[1], H. Sun[70], H.K. Sun[1], J.F. Sun[20], K. Sun[67], L. Sun[82], R. Sun[77], S.S. Sun[1,70], T. Sun[56,q], W.Y. Sun[55], Y.C. Sun[82], Y.H. Sun[32], Y.J. Sun[64,77], Y.Z. Sun[1], Z.Q. Sun[1,70], Z.T. Sun[54], H. Tabaharizato[1], C.J. Tang[59], G.Y. Tang[1], J. Tang[65], J.J. Tang[64,77], L.F. Tang[43], Y.A. Tang[82], L.Y. Tao[78], M. Tat[75], J.X. Teng[64,77], J.Y. Tian[64,77], W.H. Tian[65], Y. Tian[34], Z.F. Tian[82], I. Uman[68b], E. van der Smagt[3], B. Wang[65], Bin Wang[1], Bo Wang[64,77], C. Wang[42,c,d], Chao Wang[20], Cong Wang[23], D.Y. Wang[50,b], H.J. Wang[42,c,d], H.R. Wang[84], J. Wang[10], J.J. Wang[82], J.P. Wang[37], K. Wang[1,64], L.L. Wang[1], L.W. Wang[38], M. Wang[54], Mi Wang[64,77], N.Y. Wang[70], S. Wang[42,c,d],

JHEP06(2026)009

Shun Wang[63], T. Wang[12,e], T.J. Wang[47], W. Wang[65], W.P. Wang[39], X.F. Wang[42,c,d], X.L. Wang[12,e], X.N. Wang[1,70], Xin Wang[27,h], Y. Wang[1], Y.D. Wang[49], Y.F. Wang[1,9,70], Y.H. Wang[42,c,d], Y.J. Wang[64,77], Y.L. Wang[20], Y.N. Wang[49], Yanning Wang[82], Yaqian Wang[18], Yi Wang[67], Yuan Wang[18,34], Z. Wang[1,64], Z.L. Wang[2], Z.Q. Wang[12,e], Z.Y. Wang[1,70], Zhi Wang[47], Ziyi Wang[70], D. Wei[47], D.H. Wei[14], D.J. Wei[72], H.R. Wei[47], F. Weidner[74], S.P. Wen[1], U. Wiedner[3], G. Wilkinson[75], M. Wolke[81], J.F. Wu[1,9], L.H. Wu[1], L.J. Wu[20], Lianjie Wu[20], S.G. Wu[1,70], S.M. Wu[70], X.W. Wu[78], Z. Wu[1,64], H.L. Xia[64,77], L. Xia[64,77], B.H. Xiang[1,70], D. Xiao[42,c,d], G.Y. Xiao[46], H. Xiao[78], Y. L. Xiao[12,e], Z.J. Xiao[45], C. Xie[46], K.J. Xie[1,70], Y. Xie[54], Y.G. Xie[1,64], Y.H. Xie[6], Z.P. Xie[64,77], T.Y. Xing[1,70], D.B. Xiong[1], C.J. Xu[65], G.F. Xu[1], H.Y. Xu[2], M. Xu[64,77], Q.J. Xu[17], Q.N. Xu[32], T.D. Xu[78], X.P. Xu[60], Y. Xu[12,e], Y.C. Xu[84], Z.S. Xu[70], F. Yan[24], L. Yan[12,e], W.B. Yan[64,77], W.C. Yan[87], W.H. Yan[6], W.P. Yan[20], X.Q. Yan[12,e], Y.Y. Yan[66], H.J. Yang[56,q], H.L. Yang[38], H.X. Yang[1], J.H. Yang[46], R.J. Yang[20], X.Y. Yang[72], Y. Yang[12,e], Y.H. Yang[47], Y.M. Yang[87], Y.Q. Yang[10], Y.Z. Yang[20], Youhua Yang[46], Z.Y. Yang[78], Z.P. Yao[54], M. Ye[1,64], M.H. Ye[9,†], Z.J. Ye[61,g], Junhao Yin[47], Z.Y. You[65], B.X. Yu[1,64,70], C.X. Yu[47], G. Yu[13], J.S. Yu[27,h], L.W. Yu[12,e], T. Yu[78], X.D. Yu[50,b], Y.C. Yu[87], Yongchao Yu[42], C.Z. Yuan[1,70], H. Yuan[1,70], J. Yuan[38], Jie Yuan[49], L. Yuan[2], M.K. Yuan[12,e], S.H. Yuan[78], Y. Yuan[1,70], C.X. Yue[43], Ying Yue[20], A.A. Zafar[79], F.R. Zeng[54], S.H. Zeng[69], X. Zeng[12,e], Y.J. Zeng[1,70], Yujie Zeng[65], Y.C. Zhai[54], Y.H. Zhan[65], B.L. Zhang[1,70], B.X. Zhang[1,†], D.H. Zhang[47], G.Y. Zhang[20], Gengyuan Zhang[1,70], H. Zhang[64,77], H.C. Zhang[1,64,70], H.H. Zhang[65], H.Q. Zhang[1,64,70], H.R. Zhang[64,77], H.Y. Zhang[1,64], Han Zhang[87], J. Zhang[65], J.J. Zhang[57], J.L. Zhang[21], J.Q. Zhang[45], J.S. Zhang[12,e], J.W. Zhang[1,64,70], J.X. Zhang[42,c,d], J.Y. Zhang[1], J.Z. Zhang[1,70], Jianyu Zhang[70], Jin Zhang[52], Jiyuan Zhang[12,e], L.M. Zhang[67], Lei Zhang[46], N. Zhang[38], P. Zhang[1,9], Q. Zhang[20], Q.Y. Zhang[38], Q.Z. Zhang[70], R.Y. Zhang[42,c,d], S.H. Zhang[1,70], S.N. Zhang[75], Shulei Zhang[27,h], X.M. Zhang[1], X.Y. Zhang[54], Y. Zhang[1], Y. T. Zhang[87], Y.H. Zhang[1,64], Y.P. Zhang[64,77], Yu Zhang[78], Z.D. Zhang[1], Z.H. Zhang[1], Z.L. Zhang[38], Z.X. Zhang[20], Z.Y. Zhang[82], Zh.Zh. Zhang[20], Zhilong Zhang[60], Ziyang Zhang[49], Ziyu Zhang[47], G. Zhao[1], J.Y. Zhao[1,70], J.Z. Zhao[1,64], J.-P. Zhao[70], L. Zhao[1], Lei Zhao[64,77], M.G. Zhao[47], R.P. Zhao[70], S.J. Zhao[87], Y.B. Zhao[1,64], Y.L. Zhao[60], Y.P. Zhao[49], Y.X. Zhao[34,70], Z.G. Zhao[64,77], A. Zhemchugov[40,f], B. Zheng[78], B.M. Zheng[38], J.P. Zheng[1,64], W.J. Zheng[1,70], W.Q. Zheng[10], X.R. Zheng[20], Y.H. Zheng[70,i], B. Zhong[45], C. Zhong[20], H. Zhou[39,54,r], J.Q. Zhou[38], S. Zhou[6], X. Zhou[82], X.K. Zhou[6], X.R. Zhou[64,77], X.Y. Zhou[43], Y.X. Zhou[84], Y.Z. Zhou[20], A.N. Zhu[70], J. Zhu[47], K. Zhu[1], K.J. Zhu[1,64,70], K.S. Zhu[12,e], L.X. Zhu[70], Lin Zhu[20], S.H. Zhu[76], T.J. Zhu[12,e], W.D. Zhu[12,e], W.J. Zhu[1], W.Z. Zhu[20], Y.C. Zhu[64,77], Z.A. Zhu[1,70], X.Y. Zhuang[47], M. Zhuge[54], J.H. Zou[1]

[1] *Institute of High Energy Physics, Beijing 100049, People's Republic of China*
[2] *Beihang University, Beijing 100191, People's Republic of China*
[3] *Bochum Ruhr-University, D-44780 Bochum, Germany*
[4] *Budker Institute of Nuclear Physics SB RAS (BINP), Novosibirsk 630090, Russia*
[5] *Carnegie Mellon University, Pittsburgh, Pennsylvania 15213, U.S.A.*
[6] *Central China Normal University, Wuhan 430079, People's Republic of China*

JHEP06(2026)009

[7] Central South University, Changsha 410083, People's Republic of China
[8] Chengdu University of Technology, Chengdu 610059, People's Republic of China
[9] China Center of Advanced Science and Technology, Beijing 100190, People's Republic of China
[10] China University of Geosciences, Wuhan 430074, People's Republic of China
[11] Chung-Ang University, Seoul, 06974, Republic of Korea
[12] Fudan University, Shanghai 200433, People's Republic of China
[13] GSI Helmholtzcentre for Heavy Ion Research GmbH, D-64291 Darmstadt, Germany
[14] Guangxi Normal University, Guilin 541004, People's Republic of China
[15] Guangxi University, Nanning 530004, People's Republic of China
[16] Guangxi University of Science and Technology, Liuzhou 545006, People's Republic of China
[17] Hangzhou Normal University, Hangzhou 310036, People's Republic of China
[18] Hebei University, Baoding 071002, People's Republic of China
[19] Helmholtz Institute Mainz, Staudinger Weg 18, D-55099 Mainz, Germany
[20] Henan Normal University, Xinxiang 453007, People's Republic of China
[21] Henan University, Kaifeng 475004, People's Republic of China
[22] Henan University of Science and Technology, Luoyang 471003, People's Republic of China
[23] Henan University of Technology, Zhengzhou 450001, People's Republic of China
[24] Hengyang Normal University, Hengyang 421001, People's Republic of China
[25] Huangshan College, Huangshan 245000, People's Republic of China
[26] Hunan Normal University, Changsha 410081, People's Republic of China
[27] Hunan University, Changsha 410082, People's Republic of China
[28] Indian Institute of Technology Madras, Chennai 600036, India
[29] Indiana University, Bloomington, Indiana 47405, U.S.A.
[30a] INFN Laboratori Nazionali di Frascati, I-00044, Frascati, Italy
[30b] INFN Sezione di Perugia, I-06100, Perugia, Italy
[30c] University of Perugia, I-06100, Perugia, Italy
[31a] INFN Sezione di Ferrara, I-44122, Ferrara, Italy
[31b] University of Ferrara, I-44122, Ferrara, Italy
[32] Inner Mongolia University, Hohhot 010021, People's Republic of China
[33] Institute of Business Administration, Karachi
[34] Institute of Modern Physics, Lanzhou 730000, People's Republic of China
[35] Institute of Physics and Technology, Mongolian Academy of Sciences, Peace Avenue 54B, Ulaanbaatar 13330, Mongolia
[36] Instituto de Alta Investigación, Universidad de Tarapacá, Casilla 7D, Arica 1000000, Chile
[37] Jiangsu Ocean University, Lianyungang 222000, People's Republic of China
[38] Jilin University, Changchun 130012, People's Republic of China
[39] Johannes Gutenberg University of Mainz, Johann-Joachim-Becher-Weg 45, D-55099 Mainz, Germany
[40] Joint Institute for Nuclear Research, 141980 Dubna, Moscow region, Russia
[41] Justus-Liebig-Universitaet Giessen, II. Physikalisches Institut, Heinrich-Buff-Ring 16, D-35392 Giessen, Germany
[42] Lanzhou University, Lanzhou 730000, People's Republic of China
[43] Liaoning Normal University, Dalian 116029, People's Republic of China
[44] Liaoning University, Shenyang 110036, People's Republic of China
[45] Nanjing Normal University, Nanjing 210023, People's Republic of China
[46] Nanjing University, Nanjing 210093, People's Republic of China
[47] Nankai University, Tianjin 300071, People's Republic of China
[48] National Centre for Nuclear Research, Warsaw 02-093, Poland
[49] North China Electric Power University, Beijing 102206, People's Republic of China
[50] Peking University, Beijing 100871, People's Republic of China
[51] Qufu Normal University, Qufu 273165, People's Republic of China
[52] Renmin University of China, Beijing 100872, People's Republic of China
[53] Shandong Normal University, Jinan 250014, People's Republic of China
[54] Shandong University, Jinan 250100, People's Republic of China

JHEP06(2026)009

[55] Shandong University of Technology, Zibo 255000, People's Republic of China
[56] Shanghai Jiao Tong University, Shanghai 200240, People's Republic of China
[57] Shanxi Normal University, Linfen 041004, People's Republic of China
[58] Shanxi University, Taiyuan 030006, People's Republic of China
[59] Sichuan University, Chengdu 610064, People's Republic of China
[60] Soochow University, Suzhou 215006, People's Republic of China
[61] South China Normal University, Guangzhou 510006, People's Republic of China
[62] Southeast University, Nanjing 211100, People's Republic of China
[63] Southwest University of Science and Technology, Mianyang 621010, People's Republic of China
[64] State Key Laboratory of Particle Detection and Electronics, Beijing 100049, Hefei 230026, People's Republic of China
[65] Sun Yat-Sen University, Guangzhou 510275, People's Republic of China
[66] Suranaree University of Technology, University Avenue 111, Nakhon Ratchasima 30000, Thailand
[67] Tsinghua University, Beijing 100084, People's Republic of China
[68a] Istinye University, 34010, Istanbul, Turkey
[68b] Near East University, Nicosia, North Cyprus, 99138, Mersin 10, Turkey
[69] University of Bristol, H H Wills Physics Laboratory, Tyndall Avenue, Bristol, BS8 1TL, U.K.
[70] University of Chinese Academy of Sciences, Beijing 100049, People's Republic of China
[71] University of Hawaii, Honolulu, Hawaii 96822, U.S.A.
[72] University of Jinan, Jinan 250022, People's Republic of China
[73] University of Manchester, Oxford Road, Manchester, M13 9PL, United Kingdom
[74] University of Muenster, Wilhelm-Klemm-Strasse 9, 48149 Muenster, Germany
[75] University of Oxford, Keble Road, Oxford OX13RH, United Kingdom
[76] University of Science and Technology Liaoning, Anshan 114051, People's Republic of China
[77] University of Science and Technology of China, Hefei 230026, People's Republic of China
[78] University of South China, Hengyang 421001, People's Republic of China
[79] University of the Punjab, Lahore-54590, Pakistan
[80a] University of Turin, I-10125, Turin, Italy
[80b] University of Eastern Piedmont, I-15121, Alessandria, Italy
[80c] INFN, I-10125, Turin, Italy
[81] Uppsala University, Box 516, SE-75120 Uppsala, Sweden
[82] Wuhan University, Wuhan 430072, People's Republic of China
[83] Xi'an Jiaotong University, No.28 Xianning West Road, Xi'an, Shaanxi 710049, P.R. China
[84] Yantai University, Yantai 264005, People's Republic of China
[85] Yunnan University, Kunming 650500, People's Republic of China
[86] Zhejiang University, Hangzhou 310027, People's Republic of China
[87] Zhengzhou University, Zhengzhou 450001, People's Republic of China

[a] Also at the Novosibirsk State University, Novosibirsk, 630090, Russia
[b] Also at State Key Laboratory of Nuclear Physics and Technology, Peking University, Beijing 100871, People's Republic of China
[c] Also at MOE Frontiers Science Center for Rare Isotopes, Lanzhou University, Lanzhou 730000, People's Republic of China
[d] Also at Lanzhou Center for Theoretical Physics, Lanzhou University, Lanzhou 730000, People's Republic of China
[e] Also at Key Laboratory of Nuclear Physics and Ion-beam Application (MOE) and Institute of Modern Physics, Fudan University, Shanghai 200443, People's Republic of China
[f] Also at the Moscow Institute of Physics and Technology, Moscow 141700, Russia
[g] Also at Guangdong Provincial Key Laboratory of Nuclear Science, Institute of Quantum Matter, South China Normal University, Guangzhou 510006, China
[h] Also at School of Physics and Electronics, Hunan University, Changsha 410082, China
[i] Also at Hangzhou Institute for Advanced Study, University of Chinese Academy of Sciences, Hangzhou 310024, China

JHEP06(2026)009

[j] Also at Goethe University Frankfurt, 60323 Frankfurt am Main, Germany
[k] Also at Bogazici University, 34342 Istanbul, Turkey
[l] Currently at University of Silesia in Katowice, Institute of Physics, 75 Pulku Piechoty 1, 41-500 Chorzow, Poland
[m] Also at the NRC "Kurchatov Institute", PNPI, 188300, Gatchina, Russia
[n] Also at the Functional Electronics Laboratory, Tomsk State University, Tomsk, 634050, Russia
[o] Also at Applied Nuclear Technology in Geosciences Key Laboratory of Sichuan Province, Chengdu University of Technology, Chengdu 610059, People's Republic of China
[p] Also at Ecole Polytechnique Federale de Lausanne (EPFL), CH-1015 Lausanne, Switzerland
[q] Also at Key Laboratory for Particle Physics, Astrophysics and Cosmology, Ministry of Education; Shanghai Key Laboratory for Particle Physics and Cosmology; Institute of Nuclear and Particle Physics, Shanghai 200240, People's Republic of China
[r] Also at Helmholtz Institute Mainz, Staudinger Weg 18, D-55099 Mainz, Germany
[†] Deceased

JHEP06(2026)009